Int. J. Heat Mass Transfer. Vol. 5, pp. 825–836. Pergamon Press 1962. Printed in Great Britain.

UNSTEADY-STATE HEAT AND MASS TRANSFER IN THE ROTATING-DISK–REVOLVING-FLUID SYSTEM

DONALD R. OLANDER

Department of Nuclear Engineering,
University of California, Berkeley, California

(*Received* 15 *August* 1961 *and in revised form* 16 *February* 1962)

Abstract—The transient heat- and mass-transfer behavior of various rotating-disk–revolving-fluid combinations has been investigated. The analysis assumes steady flow and instantaneous application of a temperature or composition change at the disk at zero time. The approach of the dimensionless heat- or mass-transfer parameters, the Sherwood or Nusselt numbers, to their steady-state values has been investigated. The numerical computations for the pure rotating-disk case utilized both the true velocity profile and some limiting forms applicable to restricted regions of the Schmidt or Prandtl number and time. The results indicate that, for practical purposes, steady-state transfer is essentially instantaneously attained upon application of the new boundary condition. For $Sc \to \infty$, the effect of interfacial velocity on the transient response is small.

NOMENCLATURE

B, constant describing the linear portion of the axial velocity profile,
$f(\epsilon_v)$, ratio of the steady-state Sherwood number to that for $\epsilon_v = 0$, equation (29);
$f(\xi)$, dimensionless velocity parameter for flat-plate flow;
$g(\epsilon_v)$, defined by equation (28);
$H(\xi)$, dimensionless axial velocity, equation (3);
Nu, Nusselt number;
Pr, Prandtl number;
S, ratio of the mass flux of the second component to that of the diffusing species, at the solid surface;
s, dummy variable of integration;
Sc, Schmidt number;
Sh, Sherwood number;
T, temperature, degC;
T_1, T_2, T_3, T_4, dimensionless time variables, equations (8), (11), (15) and (22);
t, time, s;
U, main stream velocity in flat-plate flow, cm/s;
W, mass fraction of diffusing solute;
w, axial velocity, cm/s;
x, distance along a flat plate, cm;
x_2, x_3, x_4, dimensionless distance variable, equations (9), (13) and (20);
z, axial distance from disk, cm.

Greek symbols

α, coefficient of parabolic term of power series expansion of $H(\xi)$ about $\xi = 0$ equal to 0·5102;
ϵ_v, interfacial velocity parameter;
θ, dimensionless mass fraction, $(W - W_\infty)/(W_0 - W_\infty)$ or dimensionless temperature, $(T - T_\infty)/(T_0 - T_\infty)$;
ξ, dimensionless axial distance, equation (2);
ω, angular velocity, rad/s;
ν, kinematic viscosity of fluid, cm²/s.

Suffixes

0, at the disk, $\xi = 0$;
∞, at large distance from the disk, $\xi \to \infty$;
ss, steady-state value, $t \to \infty$;
$*$, for $\epsilon_v = 0$.

INTRODUCTION

THE nature of the steady flows produced by a disk rotating in an infinite body of fluid revolving at a different angular velocity from the disk

has recently been the subject of numerous investigations [1–3]. The heat-transfer problem associated with the pure rotating-disk system (stationary fluid) has been solved for all Prandtl numbers by Millsaps and Pohlhausen [4], and Sparrow and Gregg [5]. The latter authors have also investigated, by a perturbation method, the flow about an unsteadily rotating disk [6].

The purpose of this work is to present solutions of the unsteady-state energy or diffusion equations for the combined rotating-disk–revolving-fluid system. The fluid is assumed to have attained a steady flow situation and, at zero time, a unit change in temperature or composition is applied to the disk.

Cess and Sparrow [7] have investigated the rotating-disk system by means of an approximate solution to the energy equation. Although their technique gives an accurate closed-form expression for the transient behavior of the system, it is limited to Prandtl numbers between ~ 1 and 100 and requires numerical evaluation of two integrals for each Prandtl number. In this paper, the regions of very high and low Prandtl numbers will be investigated, and several explicit forms of the transient solutions will be examined. The difference between the heat- and mass-transfer processes will also be considered.

HEAT TRANSFER AND ZERO-DRIVING-FORCE MASS TRANSFER

For heat-transfer situations in which the viscous dissipation term is negligible and for mass transfer in which the mass flux is small enough to neglect the interfacial velocity term, the constant-property, unsteady-state energy or species conservation equation takes the form

$$\frac{\partial^2\theta}{\partial\xi^2} - Pr\, H(\xi)\frac{\partial\theta}{\partial\xi} = Pr\frac{\partial\theta}{\partial(\omega_0 t)}. \tag{1}$$

This relation is written for heat transfer, but replacement of the Prandtl number by the Schmidt number converts it to the diffusion equation. The dimensionless velocity and axial distance are defined by

$$\xi = z\sqrt{\left(\frac{\omega_0}{\nu}\right)} \tag{2}$$

$$H(\xi) = w/\sqrt{(\nu\omega_0)}. \tag{3}$$

The boundary conditions are

$$\theta[\xi, 0] = 0; \quad \theta[0, (\omega_0 t)] = 1 \qquad \theta[\infty, (\omega_0 t)] = 0. \tag{4}$$

Solutions of equation (1), expressed as the variation of the gradient at the disk with time, have been obtained. Since heat- or mass-transfer coefficients are proportional to the gradient at the disk, the dimensionless group involving these coefficients, i.e. the Nusselt and Sherwood numbers, will be utilized

$$Nu = -\left(\frac{\partial\theta}{\partial\xi}\right)_{\xi=0}. \tag{5}$$

The right-hand side of equation (5) refers either to the Nusselt or Sherwood number but, for consistency, the Nusselt number will be employed. The results will be presented in the form of the ratio of the Nusselt number at a dimensionless time $\omega_0 t$ to that at steady state.

When the fluid above the disk is itself in rotational motion, one boundary condition on the equations of motion is altered, and new velocity profiles must be computed for each value of the ratio ω_0/ω_∞. If the fluid at infinity is rotating at a greater speed than the disk, it is convenient to base the dimensionless transformations upon the fluid rotation rate rather than that of the disk. In this case, ω_0 in equations (1–3) is replaced by ω_∞ and the dimensionless time is $\omega_\infty t$. For a disk rotating in a stationary fluid, $\omega_0/\omega_\infty = \infty$; and for a fluid revolving over a stationary disk, $\omega_0/\omega_\infty = 0$. Axial velocity profiles for these limiting situations have been tabulated by Schlichting [8], while those for intermediate values of the parameter ω_0/ω_∞ are available from the work of Rogers and Lance [3].†

STEADY-STATE SOLUTION

With the right-hand side of equation (1) equal to zero, and the boundary conditions $\theta(0) = 1$, $\theta(\infty) = 0$, the solution for steady-state transfer can be written as

† The profiles need not be tabulated as $H(\xi)$ vs. ξ. Five constants characteristic of the flow suffice to generate an asymptotic power series from $\xi = 0$ to a chosen match point, beyond which $H(\xi)$ is represented by an exponential series [1–3].

$$Nu_{ss} = [\int_0^\infty \exp\{Pr \int_0^\xi H(s)\,ds\}\,d\xi]^{-1}. \quad (6)$$

Sparrow and Gregg [5] have obtained exact numerical solutions of equation (6) for $\omega_\infty = 0$ and a large range of Prandtl (or Schmidt) numbers. A significant characteristic of rotating-disk–revolving-fluid flows is the approach of $H(\xi)$ to a constant value at large distances from the disk. The form of equation (6) requires that $H(\infty) \leqslant 0$; otherwise, the integral increases without bound. Since the sign of $H(\infty)$ changes from negative to positive as ω_0/ω_∞ decreases below unity, we can conclude that the steady-state solution is zero when the fluid is rotating more rapidly than the disk.

In this respect the system is similar to conduction into a motionless medium, for which a steady state of zero is approached. When the fluid motion is directed away from the source, mass or energy is convected further and further into the medium as time progresses; this continually reduces the magnitude of the gradient (and hence the flux) at the surface towards zero. When the fluid moves toward the source, the continuous introduction of fresh material into the region close to the surface permits a potential gradient at the source surface to be maintained; hence a non-zero flux will persist after the transient period has died away.

UNSTEADY-STATE SOLUTIONS

Numerical solutions of equation (1) have been obtained by the method of finite differences, utilizing tabulated values or the equivalent series representations of the axial velocity profile.

For the rotating disk ($\omega_\infty = 0$), certain limiting cases of time and Pr permit simplifications in equation (1) which allow either analytical solution or a transformation which removes the explicit dependence on the Schmidt number.

Case I—Very small times, all Pr

After the temperature or composition of the disk has been suddenly altered, there will follow a period of time during which the depth of penetration into the fluid is so small that the axial velocity can be considered zero. The heat- or mass-transfer rate will follow the time dependence characteristic of conduction into a stagnant medium. With $H(\xi) \simeq 0$, the solution of equation (1) can be written as

$$\frac{Nu}{Nu_{ss}} = \frac{1}{Nu_{ss}}\sqrt{\left(\frac{1}{\pi T_1}\right)} \quad (7)$$

where

$$T_1 = \frac{\omega_0 t}{Pr}. \quad (8)$$

Nu_{ss} is computed by equation (6) using the actual velocity profile.

Case II—Large times, small Pr ($\leqslant 0{\cdot}1$)

In this case, the steady-state diffusion or thermal boundary layer is considerably greater than the hydrodynamic boundary layer [5]. For times sufficiently large such that the temperature or concentration profile is reasonably close to its steady-state value,

$$H(\xi) \simeq H(\infty) = -0{\cdot}886,$$

and with

$$x_2 = -Pr\,H(\infty)\xi \quad (9)$$

equation (1) becomes

$$\frac{\partial^2\theta}{\partial x_2^2} + \frac{\partial\theta}{\partial x_2} = \frac{\partial\theta}{\partial T_2} \quad (10)$$

where

$$T_2 = Pr[H(\infty)]^2\omega_0 t. \quad (11)$$

The solution of equation (10) is [9]

$$\frac{Nu}{Nu_{ss}} = \frac{1}{\sqrt{(\pi T_2)}}\,e^{-T_2/4} + \tfrac{1}{2}[1 + \operatorname{erf}(\tfrac{1}{2}\sqrt{T_2})] \quad (12)$$

Case III—Large times, Pr $\simeq 1$

For these Prandtl numbers, a significant portion of the concentration or temperature change falls in the region $0 \leqslant \xi \leqslant 2$, within which $H(\xi)$ is approximately linear with axial distance (see Fig. 2 of [5]). Taking $H(\xi) \simeq -B\xi$, and making the dimensionless transformation

$$x_3 = \xi\sqrt{\left(\frac{Pr\,B}{2}\right)}, \quad (13)$$

equation (1) can be written as

$$\frac{\partial^2\theta}{\partial x_3^2} + 2x_3\frac{\partial\theta}{\partial x_3} = \frac{\partial\theta}{\partial T_3} \quad (14)$$

where

$$T_3 = \tfrac{1}{2}B\omega_0 t. \tag{15}$$

The solution of equation (14), subject to boundary conditions equivalent to equation (4), is

$$\frac{Nu}{Nu_{ss}} = [1 - e^{-4T_3}]^{-\frac{1}{2}}. \tag{16}$$

To estimate the reliability of the linear-velocity assumption, the steady-state solution of equation (14) was first obtained as

$$\left(\frac{d\theta}{dx_3}\right)_0 = -\frac{2}{\sqrt{\pi}}. \tag{17}$$

Using equation (13)

$$Nu_{ss} = -\left(\frac{d\theta}{d\xi}\right)_0 = \sqrt{\left(\frac{2Pr\,B}{\pi}\right)} \tag{18}$$

with B approximately equal to 0·25, equation (18) becomes†

$$Nu_{ss} = 0{\cdot}40\sqrt{Pr}. \tag{19}$$

A comparison of the exact computation [5] and that predicted by equation (19) shows the latter to be 1 per cent high at $Pr = 1$ and 11 per cent high at $Pr = 10$. Although equation (19) is not useful as a method of accurately predicting Nu_{ss}, this agreement indicates that the linear-velocity profile is a reasonable assumption for $Pr \simeq 1$. However, equation (16) shows that since T_3 is not a function of the Prandtl number, neither is the ratio Nu/Nu_{ss}.

Case IV—All times, high Pr (>100)

For large Prandtl numbers, the thermal-boundary layer is always in the region in which $H(\xi) \simeq -a\xi^2$, where $a = -\frac{1}{2}H''(0)$ [5]. With this velocity profile and the transformation

$$x_4 = \left(\frac{aPr}{3}\right)^{1/3}\xi \tag{20}$$

equation (1) becomes

$$\frac{\partial^2\theta}{\partial x_4^2} + 3x_4^2\frac{\partial\theta}{\partial x_4} = \frac{\partial\theta}{\partial T_4} \tag{21}$$

where

$$T_4 = (a/3)^{2/3}\,Pr^{-1/3}\,\omega_0 t. \tag{22}$$

Numerical solution of equation (21) permits prediction of the time-dependent heat- or mass-transfer behavior for all $Pr > 100$.

Solutions of this type are more useful in mass rather than heat transfer, since the restriction $Sc > 100$ includes practically all binary liquids. It should be noted that the technique of Cess and Sparrow [7] is not applicable to large Schmidt or Prandtl numbers. They have utilized a modified Laplace transform of equation (1) and obtained solutions for large and small values of the transform variable. The series approximation for large times (small values of the transform variable) retains only two terms, and the success of this method for Prandtl numbers between 1 and 100 is due to the low ratio of the coefficients of the second and first terms—see equation (13) and Table 1 of [7]. The reason for the failure at low Prandtl numbers is the large value of this ratio. It can be shown that at large Prandtl numbers the ratio is proportional to the Prandtl number; hence the method is inapplicable in this region as well. Application of their technique to equation (21) yields an imaginary value of one of the coefficients (a_5 in their nomenclature).

Plots of Nu/Nu_{ss} vs. time for Cases I, II and IV will be separated according to Prandtl number, as can be seen by the appearance of this parameter in the dimensionless times defined by equations (8), (11) and (22). Equation (15) indicates that only for Case III will the Sherwood or Nusselt ratio be independent of Sc or Pr.

RESULTS

Rotating-disk flow ($\omega_\infty = 0$)

The solid lines of Figs. 1 and 2 show the approach to steady state transfer from a rotating disk. The curves for $Pr = 0{\cdot}01$, 0·1, 1, 10 and 100 were computed using the actual axial velocity profile [2, 8]; for $Pr = 1000$, the parabolic approximation to the velocity profile was used, i.e. this curve represents a solution of equation (21) with T_4 converted to $\omega_0 t$ by equation (22).

The curves of Fig. 1 shows that for low Prandtl

† The straight line has been drawn through the origin of Fig. 2, Ref. [5].

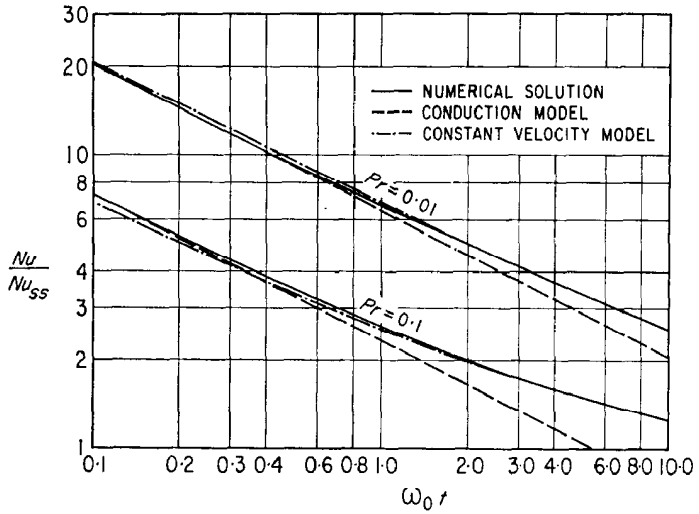

FIG. 1. Transient heat transfer from a rotating disk for $Pr = 0{\cdot}1$ and $0{\cdot}01$.

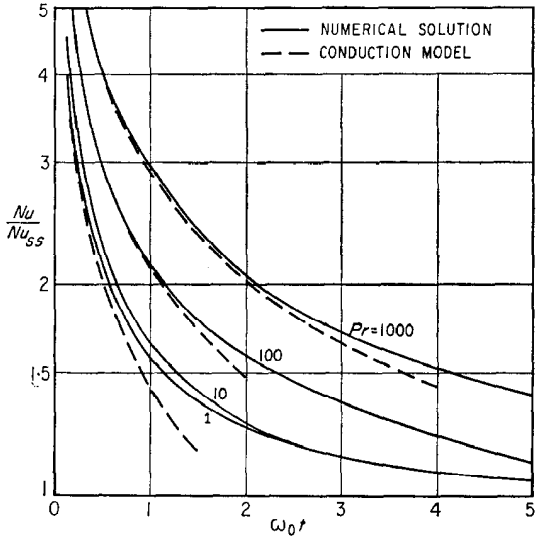

FIG. 2. Transient heat transfer from a rotating disk for $Pr = 1$, 10, 100 and 1000.

numbers the constant velocity model [equation (12)] is an excellent approximation of the actual transient behavior for all but very small times. In the region where equation (12) begins to diverge from the true curve, the conduction model takes its place as a satisfactory approximation. With appropriate matching, equations (7) and (12) reproduce the numerical solution to within ± 4 per cent at all times.

The numerical solutions for $Pr = 1$, 10 and 100 (Fig. 2) are in excellent agreement with the closed-form solution of Cess and Sparrow [7]. The conduction model follows the true curve until quite close to steady state, or for Nu/Nu_{ss}

between 2 and 3. At $\omega_0 t > 2$, the curves for $Pr = 1$ and 10 coincide, indicating that the restrictions of Case III are fulfilled. The solid curve for $Pr = 1$ is predicted by equations (15) and (16) to within 0·5 per cent.

For practical purposes, a more significant measure of transient behavior is the time required to reach a certain percentage of steady state. Fig. 3 shows the $\omega_0 t$ values required for Nu/Nu_{ss} to reach 1·5 and 1·05 as functions of Pr.

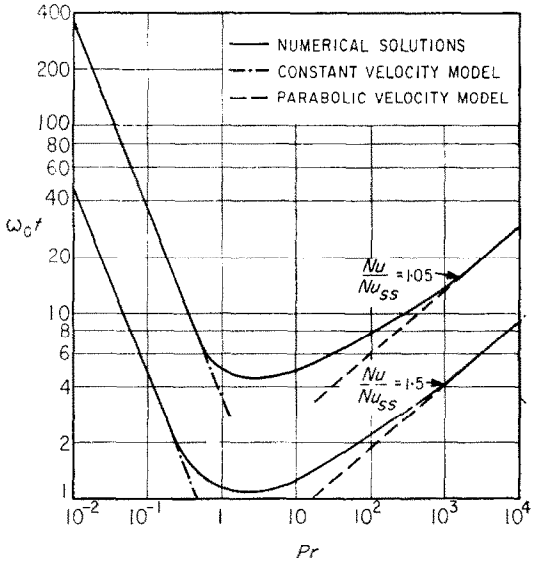

FIG. 3. Time required for various fractional approaches to steady-state, rotating disk.

The asymptotic lines for high and low Prandtl numbers have been obtained from equation (12) and the solution of equation (21). The flat minima between Prandtl numbers of 1 and 10 indicate the qualitative validity of Case III, which predicts that the time required to approach a given percentage of steady state should be independent of Prandtl number as long as the velocity profile in the region where the greatest part of the temperature or concentration change occurs is effectively linear. The true minimum is in the neighborhood of $Pr = 3$; the transient curve for this Prandtl number falls slightly below the $Pr = 1$ curve of Fig. 2 at $\omega_0 t > 2$.

This peculiar behavior of the transient response time has been noted by Cess and Sparrow [7] and is due to the particular form of the axial-velocity distribution characteristic of rotating-disk flows. The minimum can be thought of as the result of two competing effects: Large thermal or mass diffusivities (or low Sc or Pr) tend to give a quick approach to steady state; strong fluid motion in a direction opposite to the heat or mass flux tends to restrict the speed of approach to steady state. This latter effect results from the fact that heat or mass diffuse relative to the mass average velocity of the fluid. Just as a fish moves more slowly upstream against a swift current, the rate of heat or mass transport as seen by a stationary observer is proportional to the difference between the diffusional velocity (which is a function of the diffusivity–gradient product) and the (negative) convective velocity. At low Prandtl numbers, the thermal boundary layer at steady state extends quite deeply into the region far from the disk where the axial inflow is strongest. This convective restriction to rapid attainment of steady state more than overcomes the high diffusivity characteristic of low-Prandtl-number fluids, so that the net result is a sluggish approach to steady state. At high Prandtl numbers, the situation is just reversed; the velocity experienced by the diffusing heat or mass is quite small since the process occurs in a region close to the solid surface. However, the very low diffusivity predominates and the approach to steady state is slow. For intermediate Prandtl numbers, the diffusivities are sufficiently large and the hydrodynamic inflow sufficiently small in the thermal or diffusion boundary layer such that the rate of approach to steady state is more rapid than for the other two cases.

The minima of Fig. 3 should be observed for any flow system in which the axial velocity [or more precisely, the equivalent of $H(\xi)$ in equation (1)] approaches a constant negative value at large distances from the solid surface. This conditions insures that as $Pr \to 0$, equation (12) will be valid, and the response time will decrease as Pr^{-1}, as the left-hand asymptotes of Fig. 3 indicate. As $Pr \to \infty$, the velocity parallel to the solid surface in the thermal or diffusion boundary layer will eventually become linear in normal distance [this condition gives rise to the parabolic form of the coefficient of $\partial\theta/\partial x_4$ in equation (21)] [10]. When this occurs,

the right-hand asymptote of Fig. 3 will describe the transient behavior, and the time of the approach to steady state will increase as the cube root of the Prandtl number. What lies between, then, must be a minimum.

As an example of a system which contains no minimum in response curves similar to Fig. 3, consider the transient response of heat transfer from a flat plate to a step change in plate temperature. The time-dependent energy equation is given by equation (1) with $H(\xi)$ replaced by $-\frac{1}{2}f(\xi)$ and $\omega_0 t$ replaced by $t/(x/U)$. The derivative of the function $f(\xi)$ represents the ratio of the parallel velocity component to the main stream velocity (U), and ξ is the dimensionless distance commonly employed in flat-plate analysis.† For low Prandtl numbers, the thermal boundary layer is much larger than the flow boundary layer, and $f(\xi)$ can be replaced by its asymptotic form for large distances. Thus $f(\xi) = \xi + K$, where K is a constant. If x_3 is defined as $\frac{1}{2}\sqrt{(Pr)}\ (\xi + K)$ and T_3 as $t/4(x/U)$, the flat-plate energy equation reduces to equation (14). The steady-state solution is:

$$\lim_{Pr\to 0} Nu_{ss} = \sqrt{\left(\frac{Pr}{\pi}\right)} \qquad (23)$$

which is too high by 3 per cent at $Pr = 0{\cdot}001$, 8 per cent at $Pr = 0{\cdot}01$ and 22 per cent at $Pr = 0{\cdot}1$ [11]. The unsteady-state solution is:

$$\lim_{Pr\to 0}\left(\frac{Nu}{Nu_{ss}}\right) = \{1 - \exp[-t/(x/U)]\}^{-1/2}. \qquad (24)$$

At large Schmidt numbers, $f(\xi) \to 2a\xi^2$, where $a = 0{\cdot}083$ [10]. The energy equation thus reduces to equation (21).

Knowledge of these two limiting cases permits construction of asymptotic response curves similar to those of Fig. 3; these are shown on Fig. 4 for the flat-plate geometry. Rather than passing through a minimum, the transient curves approach a constant value as $Pr \to 0$, which is obtainable from equation (24). Since the range of validity of the unsteady-state asymptotic forms roughly corresponds to the applicability of their steady-state counterparts, the right-hand asymptotes of Fig. 4 should be fairly reliable down to $Pr \simeq 1$, while the low-

† For the flat plate, $\xi = y[U/\nu x]^{1/2}$, where y is distance normal to the surface.

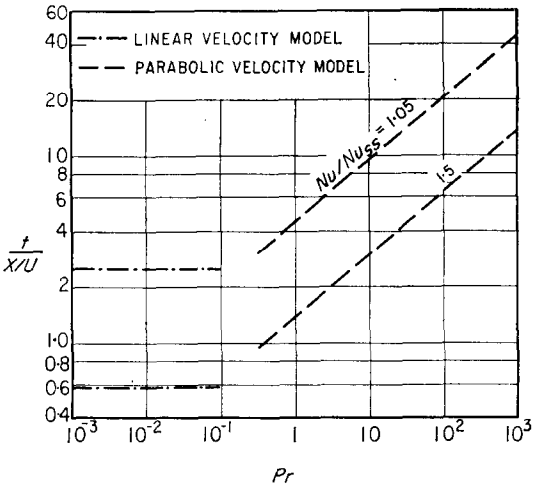

FIG. 4. Time required for various fractional approaches to steady-state, flat plate.

Prandtl-number form is probably in considerable error for $Pr > 0{\cdot}01$.

Rotating disk–revolving fluid

Solutions of the energy equation for the case of a non-zero rotational velocity of the fluid above the disk were obtained by numerical solution of equation (1) and the appropriate tabulated values of $H(\xi)$ for each ω_0/ω_∞.

Figure 5 shows the transient behavior of the Nusselt number for $Pr = 1$ and $\omega_0/\omega_\infty = 5{\cdot}54$ and 2·91. In the former case, the curve is identical with that for a pure rotating disk, which indicates that the ratio 5·54 is essentially infinite as far as the velocity profiles are concerned. Fig. 6 presents the time-dependent behavior of systems in which the bulk fluid is rotating more rapidly than the disk. For these systems, as indicated above, the Nusselt number approaches zero at large times. For $\omega_0/\omega_\infty = 0{\cdot}032$ (which closely represents the rotational motion of a large body of fluid over a stationary surface) and a fluid rotational rate of 10 s^{-1}, the Nusselt number is 0·03 after $\frac{1}{2}$ s. By comparison, the Nusselt number for a disk rotating at 10 s^{-1} in a stationary fluid is 0·41 after $\frac{1}{2}$ s.

Figures 5 and 6 indicate that, as ω_0/ω_∞ approaches unity, the transient response becomes slower. This is due to the increasing size of the hydrodynamic and thermal boundary layers as the state of solid rotation is approached.

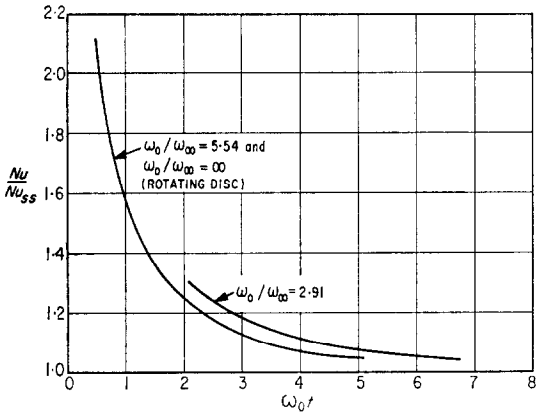

FIG. 5. Transient heat transfer of rotating-disk–revolving-fluid combination, $\omega_0/\omega_\infty > 1$, $Pr = 1$.

At $\omega_0/\omega_\infty = 1$, there is no gross fluid motion, and the system is one of pure conduction or diffusion, for which the "boundary layers" are infinite in extent. Any convective contribution to energy or material transport, whether it be flow toward the disk ($\omega_0/\omega_\infty > 1$) or outflow ($\omega_0/\omega_\infty < 1$), results in a more rapid response than that of pure conduction or diffusion.

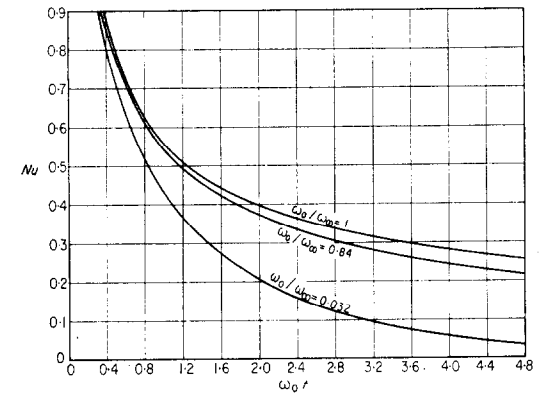

FIG. 6. Transient heat transfer behavior of rotating-disk–revolving-fluid combination, $\omega_0/\omega_\infty < 1$, $Pr = 1$.

Unsteady-state mass transfer at high rates

The preceding development of the transient behavior of the rotating-disk system is applicable only to those mass-transfer situations in which the driving force or the mass flux is small. If this is not so, the axial velocity at the disk surface generated by the mass-transfer process cannot be neglected, and its effect on boundary conditions of the equations of motion must be considered. An exact solution represents a formidable problem, for not only are three non-linear, time-dependent, hydrodynamic equations coupled to equation (1), but the axial velocity boundary condition at the disk, $H(0)$, is non-zero and varies with time as well. In order to estimate the effect of the interfacial velocity upon the transient behavior which has been developed for heat transfer and zero-driving-force mass transfer, two limiting cases will be considered: (1) a short-time approximation equivalent to the pure conduction model considered previously and valid for all Schmidt numbers, and (2) a long-time approximation for high Schmidt numbers.

Immediately following a step change in concentration at the disk, the mass-transfer process resembles that of pure diffusion into a motionless medium. The only convective motion in the fluid is that resulting from the movement of the diffusing species itself and can be related to the gradient at the disk by [10]:

$$H(0) = -\frac{\epsilon_v}{Sc}\left(\frac{\partial\theta}{\partial\xi}\right)_0 \tag{25}$$

where

$$\epsilon_v = \frac{W_0 - W_\infty}{[1/(1+S)] - W_0} \tag{26}$$

and S represents the ratio of the mass fluxes of the second component to that of the diffusing species. If the second component is not transferred across the disk surface, $S = 0$, and equation (26) represents the "stagnant B" condition commonly encountered in mass-transfer analyses. Equations (25) and (26) arise directly from the definition of a Maxwell–Stephan or Chapman–Cowling type diffusion coefficient [10]. In the following analysis, the properties of the mixture (e.g. viscosity, density and diffusivity) will be assumed independent of composition. The effect of variable properties on the steady-state transfer is not large, at least for high Schmidt number systems [10].

With the hydrodynamic velocity approximated by equation (25) for short times, equation (1) becomes

$$\frac{\partial^2\theta}{\partial\xi^2} + \epsilon_v\left(\frac{\partial\theta}{\partial\xi}\right)_0\frac{\partial\theta}{\partial\xi} = Sc\,\frac{\partial\theta}{\partial(\omega_0 t)}. \tag{27}$$

Following the development of Bird *et al.* [12], the solution to equation (27) can be written as

$$g(\epsilon_v) = Sh\sqrt{(\pi T_1)} = \frac{\exp\{-\epsilon_v^2 Sh^2 T_1\}}{1 + \text{erf}\{\epsilon_v Sh\sqrt{T_1}\}} \quad (28)$$

where Sh represents the gradient at the disk [the right-hand side of equation (5)] and T_1 is given by equation (8).† As $\epsilon_v \to 0$, $g(\epsilon_v)$ approaches unity, and equation (28) reduces to equation (7). The solution of equation (28) is presented on Fig. 7 as the $g(\epsilon_v)$ vs. ϵ_v curve. Equation (28) indicates that the effect of interfacial velocity on the short-time transient behavior is simply a displacement of the conduction-type curves by the factor $g(\epsilon_v)$. However, in order to express the results as the ratio

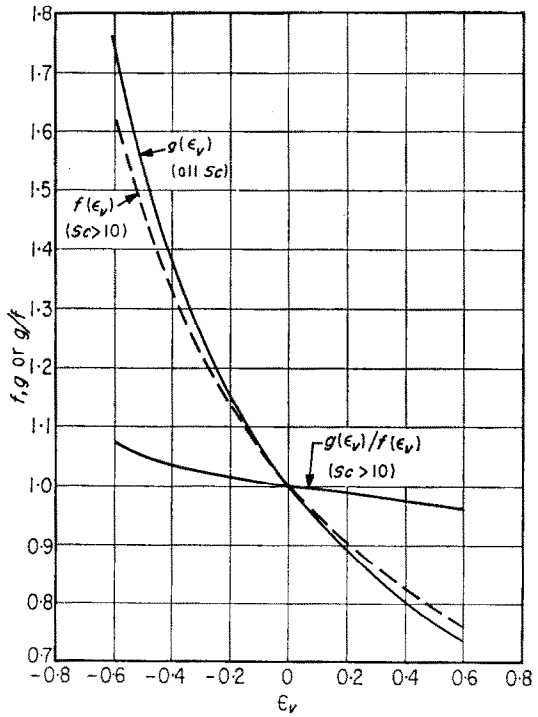

FIG. 7. The effect of interfacial velocity on the diffusion model for transient mass transfer.

Sh/Sh_{ss}, the effect of ϵ_v on the steady-state Sherwood number must also be considered. This effect has been investigated elsewhere [13], and the results can be represented by

$$\frac{Sh_{ss}}{Sh_{ss}^*} = f(\epsilon_v) \quad (29)$$

where Sh_{ss}^* denotes the steady-state Sherwood number in the absence of interfacial velocity and is equal to the steady-state Nusselt number which has been used in the preceding section. The function $f(\epsilon_v)$ can be obtained from a cross plot of the curves of the figure in [13]. In general, $f(\epsilon_v)$ is a function of Schmidt number, but this dependency ceases for $Sc > 10$. Combining equations (28) and (29), the exact mass-transfer analog of equation (7) can be written as

$$\frac{Sh}{Sh_{ss}} = \left[\frac{g(\epsilon_v)}{f(\epsilon_v)}\right] \frac{1}{Sh_{ss}^*} \sqrt{\left(\frac{1}{\pi T_1}\right)}. \quad (30)$$

This relation is applicable to all Schmidt numbers, and its range of validity will probably be close to that of equation (7), i.e., until Sh/Sh_{ss} is between 2 and 3. Except for large Schmidt numbers, $f(\epsilon_v)$ must be evaluated at the particular Schmidt number in question. For all Schmidt numbers, however, the ratio $g(\epsilon_v)/f(\epsilon_v)$ differs surprisingly little from unity. For $Sc = 1$, for example, it is 1·13 at $\epsilon_v = -0{\cdot}6$ and 0·93 at $\epsilon_v = +0{\cdot}6$.‡ For $Sc > 10$, the effect is even less pronounced. The function $f(\epsilon_v)$ and the ratio $g(\epsilon_v)/f(\epsilon_v)$ are shown in Fig. 7 for $Sc > 10$. The ratio $g(\epsilon_v)/f(\epsilon_v)$ varies from 1·07 at $\epsilon_v = -0{\cdot}6$ to 0·96 for $\epsilon_v = 0{\cdot}6$.

For large Schmidt numbers, it is convenient to recast equation (30) into the time variable T_4 of equation (22). With the parabolic velocity profile assumption, Sh_{ss}^* can be obtained directly from equation (6) as $(\alpha Sc/3)^{1/3}/\Gamma(4/3)$ and equation (30) written as

$$\frac{Sh}{Sh_{ss}} = \left[\frac{\Gamma(4/3)}{\sqrt{\pi}}\right] \left[\frac{g(\epsilon_v)}{f(\epsilon_v)}\right] \frac{1}{\sqrt{T_4}}. \quad (31)$$

Here $\Gamma(4/3)$ denotes the gamma-function of 4/3.

At large Schmidt numbers, the steady-state Sherwood number can be accurately approximated by use of a velocity profile which is the sum of two contributions: the mass transfer induced interfacial velocity and the parabolic

† For the following dicusssion, Nu and Pr in equations (5-8) are replaced by Sh and Sc.

‡ For a stagnant second component ($S = 0$), $\epsilon_v = -0{\cdot}6$ represents a solute whose mass fraction is 0·6 in the bulk and zero at the disk. $\epsilon_v = 0{\cdot}6$ characterizes a solute with a mass fraction of 0·375 at the disk and zero in the bulk.

term representing the velocity distribution within the diffusion boundary layer in the no-mass-transfer system [13]. Thus, as $Sc \to \infty$,

$$H(\xi) \simeq H(0) - a\xi^2. \tag{32}$$

This approximation is satisfactory for steady-state transfer because the interfacial velocity becomes increasingly smaller as the Schmidt number increases.† In the limit as $Sc \to \infty$, the radial shear stress at the disk [which is proportional to a in equation (32)] is no longer affected by the mass-transfer process, and the velocity distribution is simply a translation of the no-mass-transfer profile by an amount $H(0)$.

In the transient case, however, two additional limitations arise:

(1) Equation (32) applies to a steady-state situation. In the transient case, the coefficient a would in general be a function of time, and higher-order terms may be significant. However, on physical grounds it can be argued that if the boundary condition $H(0)$ is a slowly varying function of time, the velocity distribution can be assumed to pass through a series of instantaneous quasi-steady states, each represented by equation (32). In this case, a would retain its no-mass-transfer value of 0·51 and the entire time variation of the axial velocity would be contained in the $H(0)$ term. There is some justification for the assumption from the study of Sparrow and Gregg [6], which was concerned with the deviation of the instantaneous torque on a rotating disk during start-up from its quasi-steady-state value. Deviations were expressed as a power series involving the time rate of change of the angular speed of the disk and its derivative. The slower the rate of change of disk speed, the better is the quasi-steady-state assumption. In an illustrative example, they showed that, for a reasonable approach of the rotational speed to its steady-state value, the quasi-steady approximation was valid by the time the disk had attained but 10 per cent of its steady-state rotational rate. The situation here is different in that the axial velocity boundary condition, rather than the tangential component, is time dependent. In addition, the time variation of $H(0)$ is not *a priori* specifiable, for it is embedded in the transient diffusion equation.

(2) Since $H(0)$ is determined by the magnitude of the composition gradient at the disk surface, equation (32) would apply only when the Sherwood number is close to its steady-state value. Otherwise, the interfacial velocity will be large enough to affect the shear stress at the disk, and the coefficient a will be correspondingly altered. This restriction is far less severe than the first, for if the region of applicability of equation (32) is restricted to time such that $Sh/Sh_{ss} < 2$, $H(0)$ will be no more than twice its steady-state value. The limitation to long times is required for the first restriction as well, since, as $t \to \infty$, the time rate of change of the Sherwood number [or $H(0)$] approaches zero.

In sum, the following assumptions will be made. The axial velocity obtained from a complete solution of the coupled unsteady-state equations of species conservation and motion can be expressed in terms of a power series in ξ, of which equation (32) represents the first two terms. By analogy to the steady-state solution, all terms involving powers of ξ greater than 2 are negligible at large Schmidt numbers. The coefficient a is in general a function both of time and of the magnitude of the interfacial velocity. At large times, or $Sh/Sh_{ss} \to 1$, the effect of $H(0)$ upon a disappears because of the small magnitude of the interfacial velocity, and the dependence on time is removed because of the slow rate of change of $H(0)$ with time. This last assumption implies quasi-steady-state hydrodynamics and true unsteady-state diffusion. It might be regarded as a "pipe-flow" assumption, since it implies that any change in the velocity of an incompressible fluid at the inlet (the disk surface) is immediately felt throughout the pipe (the diffusion boundary layer).

Inserting equations (25) and (32) into equation (1) and using equations (20) and (22), the diffusion equation valid for large Schmidt numbers at long times becomes

$$\frac{\partial^2\theta}{\partial x_4^2} + \left[\epsilon_v\left(\frac{\partial\theta}{\partial x_4}\right)_0 + 3x_4^2\right]\frac{\partial\theta}{\partial x_4} = \frac{\partial\theta}{\partial T_4}. \tag{33}$$

This relation reduces to equation (27) for short times when the depth of penetration is so

† At $Sc = 1000$ and $\epsilon_v = 0{\cdot}6$, $H(0) \simeq 0{\cdot}0033$, compared to $H(\infty) = -0{\cdot}886$.

small that the first term in the brackets overshadows the second. However, this does not imply that equation (33) is applicable at intermediate times, because of the restrictions discussed above. Plots of the solutions of equation (33) for $\epsilon_v = -0{\cdot}6$, 0·6 and 0 are shown in Fig. 8, along with the short-time diffusion approximation, equation (30). For $\epsilon_v = 0$, equation (33) reduces to equation (21), which is valid at all times for high Schmidt numbers. The solution of equation (33) for $\epsilon_v = \pm 0{\cdot}6$ has been limited to $Sh/Sh_{ss} \geqslant 1{\cdot}25$, because of its restricted applicability to long times. The $\epsilon_v = -0{\cdot}6$ curve is practically coincidental with the no-mass-transfer results. By comparison

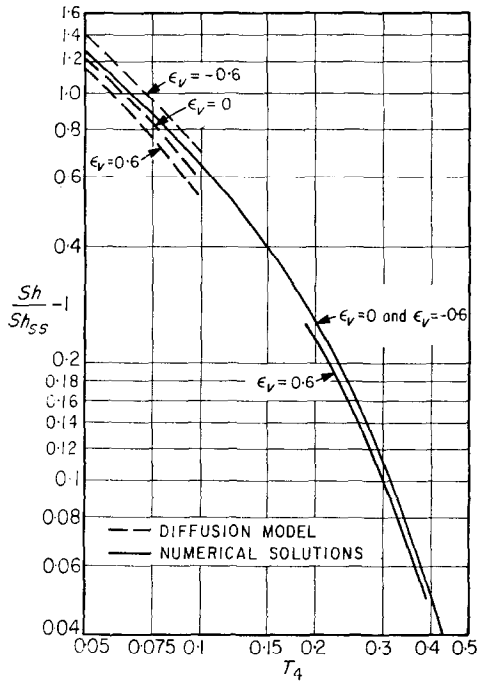

FIG. 8. Transient mass transfer as a function of ϵ_v.

of the short- and long-time approximations, it appears reasonable that the transient behavior for $\epsilon_v \neq 0$ could be sketched roughly parallel to the $\epsilon_v = 0$ curve without serious error. The most striking result of these curves is the relatively insignificant effect of the interfacial velocity on the transient behavior of the system. The times required to approach 5 per cent of steady state are within 4 per cent of each other for $-0{\cdot}6 \leqslant \epsilon_v \leqslant 0{\cdot}6$. Although no long-time approximation for the low Sc region has been obtained, the diffusion model curves for $\epsilon_v \neq 0$ are still quite close to the heat conduction analog ($\epsilon_v = 0$). For practical purposes, it can be tentatively concluded that the mass-transfer-induced interfacial velocity has a negligible effect on the transient response, and that the simple heat-transfer results are applicable to all but very high flux (large ϵ_v) mass-transfer processes.

It should be noted that the curves of Fig. 8 are not restricted to a rotating-disk geometry. At large Schmidt numbers, equation (30) [and in particular the function $f(\epsilon_v)$] applies to a flat plate [13] and probably to other geometries as well. It has also been shown that equation (32) is valid for a wide class of laminar flows [10]. Only the magnitude of the coefficient α differs with geometry, and since this parameter is removed by the transformation of equation (20), the validity of the solution of equation (33) is not restricted to the rotating-disk system.

CONCLUSIONS

Transient heat- and mass-transfer phenomena can be reasonably well predicted by the use of a number of simplified forms of the axial velocity profile, each applicable to a certain Schmidt or Prandtl number and time range. The most significant fact to be drawn from the computations is the rapidity with which the steady state is approached for most systems. For a disk rotating at 100 s^{-1} in air, for example, the heat- or mass-transfer rate is within 5 per cent of its steady-state value after 5 ms. Even for a disk rotating at 10 s^{-1} in a medium of Schmidt or Prandtl number of 5000, the 5 per cent approach is attained after 2·3 s. For a disk rotating at 10 s^{-1} in a liquid metal of $Pr = 0{\cdot}01$, however, over $\frac{1}{2}$ min is required before the heat-transfer rate is within 5 per cent of its steady value. All of the above calculations assume the instantaneous application of the new temperature or composition to the disk at zero time. Since this is not practically possible, the computed approaches to the steady state will be somewhat more rapid than the behavior of real systems. Before the transient heat or mass transfer has

begun, the flow has been assumed at its steady-state condition; the combination of transient heat or mass transfer and flow has not been considered. Approximate considerations of the interfacial velocity peculiar to mass transfer suggest that for large Schmidt numbers this effect does not markedly alter the direct application of the heat-transfer results to mass-transfer situations.

ACKNOWLEDGEMENT

The author would like to thank Alan Emanuel for his assistance, and the Lawrence Radiation Laboratory for providing the necessary computer time.

REFERENCES

1. U. T. Bodewadt, *Z. Angew. Math. Mech.* **20**, 241 (1940).
2. W. G. Cochran, *Proc. Camb. Phil. Soc.* **30**, 365 (1934).
3. M. H. Rogers and G. N. Lance, *J. Fluid Mech.* **7**, 617 (1960).
4. K. Millsaps and K. Pohlhausen, *J. Aero Space Sci.* **19**, 120 (1952).
5. E. M. Sparrow and J. L. Gregg, *Trans. ASME J. Heat Transfer*, **C81**, 249 (1959).
6. E. M. Sparrow and J. L. Gregg, *J. Aero Space Sci.* **27**, 252 (1960).
7. R. D. Cess and E. M. Sparrow, 1961 *Int. Heat Transfer Conf., Boulder, Colo.*, p. 468 (1961).
8. H. Schlichting, *Boundary Layer Theory* (4th Ed.) pp. 83, 176. McGraw-Hill, New York (1960).
9. H. S. Carslaw and J. C. Jaeger, *Conduction of Heat in Solids* (2nd Ed.) p. 388, Clarendon Press, Oxford (1959).
10. D. R. Olander, *Inst. J. Heat Mass Transfer.* **5**, 765–780 (1962).
11. E. M. Sparrow and J. L. Gregg, *J. Aero Space Sci.* **24**, 852 (1957).
12. R. B. Bird and W. E. Stewart and E. N. Lightfoot, *Transport Phenomena* p. 594. Wiley, New York (1960).
13. D. R. Olander, *Trans. ASME J. Heat Transfer.* C84, 185 (1962).

Résumé—Les transports de chaleur et de masse ont été étudiés en régime transitoire pour des ensembles variés de disques en rotation dans des fluides en mouvement. L'étude suppose l'écoulement stationnaire et l'application instantanée d'une température ou d'une variation de composition sur le disque au temps zéro. On a étudié comment les paramètres sans dimensions de transport de chaleur et de masse, les nombres de Nusselt ou de Sherwood, tendent vers les valeurs qu'ils prennent en régime permanent. Pour les calculs numériques dans le cas d'un disque en rotation simple on a utilisé à la fois le profil des vitesses vrai et quelques formes limites applicables à des domaines limités du nombre de Prandtl ou de Schmidt et limités dans le temps. Les résultats montrent que, en pratique, l'échange en régime permanent est atteint presqu'instantanément en appliquant la nouvelle condition aux limites. Pour $Sc \to \infty$, l'effet de la vitesse à l'interface sur la réponse transitoire est faible.

Zusammenfassung—Für verschiedene Kombinationen aus rotierender Scheibe und umlaufender Flüssigkeit wurde das instationäre Wärme- und Stoffübergangsverhalten untersucht. Die Analyse verlangt gleichmässige Strömung und Änderung der Temperatur oder der Stoffzusammensetzung an der Scheibe zur Zeit Null. Die Annäherung der dimensionslosen Wärme- und Stoffübergangsparameter, der Nusselt- und Sherwood-Zahl an ihre Werte im stationären Fall wurde versucht. Die numerischen Berechnung für die rotierende Scheibe allein, stützten sich sowohl auf das wirkliche Geschwindigkeitsprofil als auch auf einige Grenzformen, wie sie auf Teilbereiche der Schmidt- und Prandtl-Zahl und der Zeit anwendbar sind. Die Ergebnisse zeigen, dass für praktische Anwendungen der stationäre Übergang im wesentlichen sofort nach Einsetzen der neuen Grenzbedingungen erhalten wird. Für $Sc \to \infty$ erweist sich der Einfluss einer Zwischenflächengeschwindigkeit auf das instationäre Verhalten als klein.

Аннотация—Исследован процесс тепло-и массообмена при различных комбинациях системы «вращающийся диск-вращающаяся жидкость». В анализе предполагается, что поток стационарный, а мгновенные изменения температуры и состава жидкости на диске происходят в начальный момент времени. Рассматривается приближение безразмерных параметров переноса тепла и массы (критерии Шервуда или Нуссельта) к их значениям при стационарном процессе. В численных расчётах используются как истинный профиль скорости, так и его частные формы, пригодные к определенным областям критерия Шмидта или Прандтля и промежуткам времени. Результаты показывают, что стационарный перенос устанавливается практически сразу же после изменения граничного условия. При $Sc \to \infty$ на поверхности раздела влияние скорости на характеристику переходного режима незначительно.